AMERICAN SOCIETY FOR MICROBIOLOGY | Journal of Bacteriology®

RESEARCH ARTICLE

Mutational Analysis of Residues in PriA and PriC Affecting Their Ability To Interact with SSB in *Escherichia coli* K-12

Anastasiia N. Klimova,[a] Steven J. Sandler[a,b]

[a]Molecular and Cellular Biology Program, University of Massachusetts Amherst, Amherst, Massachusetts, USA
[b]Department of Microbiology, University of Massachusetts Amherst, Amherst, Massachusetts, USA

ABSTRACT *Escherichia coli* PriA and PriC recognize abandoned replication forks and direct reloading of the DnaB replicative helicase onto the lagging-strand template coated with single-stranded DNA-binding protein (SSB). Both PriA and PriC have been shown by biochemical and structural studies to physically interact with the C terminus of SSB. *In vitro,* these interactions trigger remodeling of the SSB on ssDNA. *priA341*(R697A) and *priC351*(R155A) negated the SSB remodeling reaction *in vitro*. Plasmid-carried *priC351*(R155A) did not complement *priC303*::*kan*, and *priA341*(R697A) has not yet been tested for complementation. Here, we further studied the SSB-binding pockets of PriA and PriC by placing *priA341*(R697A), *priA344*(R697E), *priA345*(Q701E), and *priC351*(R155A) on the chromosome and characterizing the mutant strains. All three *priA* mutants behaved like the wild type. In a Δ*priB* strain, the mutations caused modest increases in SOS expression, cell size, and defects in nucleoid partitioning (Par$^-$). Overproduction of SSB partially suppressed these phenotypes for *priA341*(R697A) and *priA344*(R697E). The *priC351*(R155A) mutant behaved as expected: there was no phenotype in a single mutant, and there were severe growth defects when this mutation was combined with Δ*priB*. Analysis of the *priBC* mutant revealed two populations of cells: those with wild-type phenotypes and those that were extremely filamentous and Par$^-$ and had high SOS expression. We conclude that *in vivo*, *priC351*(R155A) identified an essential residue and function for PriC, that PriA R697 and Q701 are important only in the absence of PriB, and that this region of the protein may have a complicated relationship with SSB.

IMPORTANCE *Escherichia coli* PriA and PriC recruit the replication machinery to a collapsed replication fork after it is repaired and needs to be restarted. *In vitro* studies suggest that the C terminus of SSB interacts with certain residues in PriA and PriC to recruit those proteins to the repaired fork, where they help remodel it for restart. Here, we placed those mutations on the chromosome and tested the effect of mutating these residues *in vivo*. The *priC* mutation completely abolished function. The *priA* mutations had no effect by themselves. They did, however, display modest phenotypes in a *priB*-null strain. These phenotypes were partially suppressed by SSB overproduction. These studies give us further insight into the reactions needed for replication restart.

KEYWORDS DNA replication, DNA replication restart, homologous recombination, DNA repair, bacteria

DNA replication is a demanding task, made so by the sheer amount of DNA to be copied, millions to billions of base pairs per cell, and the fact that cellular metabolism places many obstacles in its way: transcription complexes and different types of DNA damage often cause replication fork collapse. The need for near-perfect copies of the genome to be passed to future generations prompted evolution of efficient ways of repairing broken replication forks and then restarting them (1–3). A

Citation Klimova AN, Sandler SJ. 2020. Mutational analysis of residues in PriA and PriC affecting their ability to interact with SSB in *Escherichia coli* K-12. J Bacteriol 202:e00404-20. https://doi.org/10.1128/JB.00404-20.

Editor Thomas J. Silhavy, Princeton University

Address correspondence to Steven J. Sandler, sandler@microbio.umass.edu.

Received 13 July 2020
Accepted 1 September 2020
Accepted manuscript posted online 8 September 2020
Published 4 November 2020

key molecule in these reactions and in most DNA transactions (DNA replication, repair, and recombination) is the single-stranded-DNA-binding protein (SSB). It protects ssDNA from the chemical insults cellular metabolism may hurl at it while the DNA is being processed. Studies have shown that it is able to recruit many proteins to the DNA and that these partner proteins often help to remodel the SSB and/or ssDNA so that the DNA transaction can move forward (4, 5).

Escherichia coli SSB is a homotetramer. Each monomer has three parts: an N-terminal DNA binding core containing an oligonucleotide/oligosaccharide binding (OB) fold, an intrinsically disordered linker region and the C-terminal acidic tip (6–8). SSB can bind ssDNA in at least two major modes. The first is the SSB_{65} mode, where the ssDNA is wrapped around all four SSB monomers, and the second is the SSB_{35} mode, where only two of the four SSB monomers on average interact with the ssDNA (9, 10; reviewed in references 4 and 5). Biochemical and biophysical studies suggest that the SSB_{65} mode is favored in DNA repair and recombination (11, 12), whereas the SSB_{35} mode is favored in DNA replication (13, 14).

The last 9 residues of the SSB C terminus form a structure often referred to as the acidic tip. In addition to acidic residues, it also has hydrophobic amino acid residues. It is evolutionarily conserved among SSBs from different members of the *Bacteria* (15). In *E. coli*, sequence changes to this tip affect cell viability (16–18). It is proposed that SSB uses this structure to recruit more than a dozen proteins to the DNA (4). Structural studies reveal that several of these partner proteins have SSB-binding pockets: PriA (19), PriC (20), RecO (21), RecQ (22), RNase HI (23), the polymerase III (Pol III) χ subunit (24), and exonuclease I (ExoI) (15). The pockets of these proteins have amino acid residues that envelop the SSB F177 residue (a critical residue in the acidic tip). Mutations of the amino acid residues in these pockets cause perturbations in the interactions of these binding partners with SSB *in vitro* (15, 19–24).

Two large-scale proteomic screens and subsequent work identified at least 14 genome maintenance proteins that interact with SSB (25, 26; reviewed in references 4 and 5). Two of these SSB-interacting partners are the replication restart proteins (RRP) PriA and PriC. PriA and PriC are necessary to restart a repaired replication fork away from the origin of DNA replication in a structure-specific and cell cycle-independent manner. PriA, PriB, PriC, and DnaT combine to form three biochemically and genetically distinct pathways of replication restart called PriA-PriB, PriA-PriC, and PriC (27). A key feature of these pathways is the ability to recognize a repaired fork and remodel it to liberate a region of ssDNA so that the DnaC protein can load the DnaB replicative helicase onto the lagging-strand template at the point of the fork in the proper orientation.

PriA-SSB interactions has been extensively studied (28, 29). Crystallization of the *Klebsiella pneumoniae* PriA with a peptide comprising the acidic tip of SSB revealed that the tip is bound in an evolutionarily conserved pocket in PriA (19). The SSB-binding pocket of PriA is located at the interface of the 3′-OH DNA binding domain, the C-terminal domain, and the helicase core (Fig. 1A). It has been proposed that R697 and Q701 residues within the PriA pocket interact with the SSB tip (Fig. 1A). *E. coli* PriA R697 was analyzed *in vitro* for its importance in the PriA interaction with SSB using a single-molecule fluorescence resonance energy transfer (smFRET) assay that distinguishes between SSB binding modes. Bhattacharyya and colleagues demonstrated that PriA stabilized the SSB_{35} binding mode, whereas a PriA341(R697A) mutant failed to alter SSB-DNA complexes (19). Taken together, these data support the idea that PriA R697 is important for the ability of PriA to be recruited to the ssDNA and remodel SSB.

PriC was shown to be an SSB-interacting partner through a dual tandem affinity purification-based proteomic screen and subsequent yeast two-hybrid assay (30). PriC R121 and R155 are two arginine residues of 25 tested that were found to be required for PriC's interaction with the SSB C terminus using the yeast two-hybrid assay and isothermal titration calorimetry (30). A nuclear magnetic resonance (NMR) structure of *Cronobacter sakazakii* PriC sharing 41% sequence identity with *E. coli* PriC revealed that PriC R121 and R155 were on adjacent α-helices, on a single face of the protein. This is

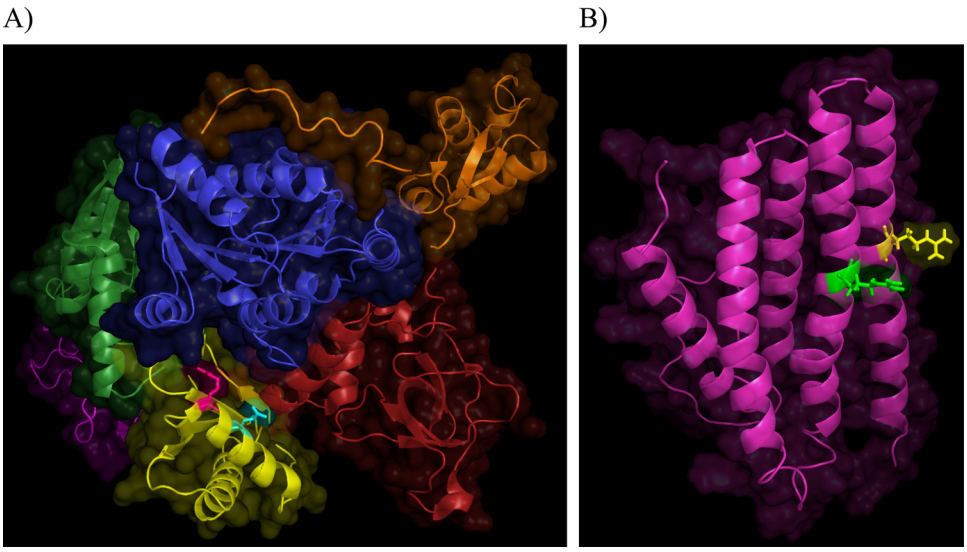

FIG 1 (A) Domain organization of *Klebsiella pneumoniae* PriA helicase as determined by X-ray crystallography (PDB code 4NL4). PriA architecture includes an N-terminal DNA-binding domain and a C-terminal helicase domain. The DNA-binding domain is divided into a 3′-DNA-binding domain (red) and a winged helix (orange). The helicase domain is composed of a helicase lobe 1 (blue) and lobe 2 (green). Two elements within lobe 2 include a Cys-rich region (purple) and a C-terminal domain (yellow). Residues involved in SSB binding are Arg-697 (magenta) and Gln-701 (cyan). (B) NMR structure of a full-length PriC protein from *Cronobacter sakazakii* (PDB code 2NCJ). Residues stabilizing its interaction with SSB are Arg-121 (green) and Arg-151 (yellow), which correspond to residues Arg-121 and Arg-155 of *E. coli* PriC.

consistent with the idea that these two basic side chains are in close proximity and mediate an interaction with SSB (20) (Fig. 1B). Both *E. coli priC*(R121A) and *priC351*(R155A) mutations expressed from a plasmid did not complement a *priC303*::*kan* chromosomal null mutation (30). Using an smFRET assay as described above for the PriA-SSB interaction, PriC was shown to be recruited to the ssDNA substrate and stabilized the SSB_{35} binding mode, whereas the PriC351(R155A) mutant protein failed to alter the SSB-DNA complexes (30). Together, these results demonstrate that PriC R155 is required for PriC binding to SSB and is important for PriC function both *in vitro* and *in vivo*.

In this work, we further investigated whether PriA and PriC residues identified as being important in the smFRET assay *in vitro* for interactions with SSB are essential for PriA and PriC function *in vivo*. To do this, we placed mutated *priA* and *priC* genes on the chromosome at their endogenous loci under regulation from their native promoters. Similar to *priC303*::*kan*, *priC351*(R155A) caused *priA* null-like phenotypes in Δ*priB* strains. In contrast, three single *priA* mutations in the SSB-binding pocket, *priA341*(R697A), *priA344*(R697E), and *priA345*(Q701E), were not sufficient to produce any noticeable phenotype *in vivo* in an otherwise wild-type cell. In Δ*priB* strains, however, all three mutations caused modest negative changes in several phenotypes tested. SSB overproduction could partially suppress these negative phenotypes for two of the three *priA* mutations. The data are consistent with the PriC R155 residue being important for SSB interactions and remodeling *in vivo*. It appears, however, that PriA has abilities similar to those of PriC to interact with and remodel SSB *in vitro*. While it is not clear yet exactly how PriA modulates SSB to efficiently help the restart process, it is clear that the role of PriA R697 and Q701 in SSB interactions and remodeling is more complicated than that of PriC R155, as they have a greater effect in the PriA-PriC pathway than in the PriA-PriB pathway.

RESULTS

It was previously shown that defects in replication restart mutants can be characterized by changes in cell viability, UV resistance, recombination ability, basal levels of

TABLE 1 Phenotypic characterization of three *priA* mutations within the SSB-binding pocket

Strain	Mutation	Avg cell area (pixels)[a,b]	SOS expression (RFI)[b,c]	Partitioning ability[d]	Cell count
SS6321	+	572 ± 6	2.23 ± 0.04	++	758
SS11228	*priA341*(R697A)	548 ± 5	2.45 ± 0.07	++	1,103
SS11245	*priA344*(R697E)	644 ± 7	2.50 ± 0.08	++	1,005
SS11244	*priA345*(Q701E)	567 ± 5	2.26 ± 0.04	++	1,274
SS7064	*priA2*::*kan*	2,157 ± 161	13.80 ± 0.80	−	342

[a]Cells were grown as described in Materials and Methods. One pixel is equal to 0.0625 μm according to our microscopic parameters. The standard errors of the means for the entire cell population are shown.

[b]Statistical analysis was done using Student's *t* test. The average cell areas of the *priA341* (SS11228) and the *priA344* (SS11245) strains are significantly different from that of the wild type (SS6321) ($P < 0.005$ and $P < 0.001$, respectively). The average cell area of the *priA345* (SS11244) mutant is not significantly different from that of the wild type ($P = 0.6$). The differences in level of SOS expression between the *priA341* and the *priA344* mutants and the wild type are significant ($P < 0.01$ and $P < 0.005$, respectively). The level of SOS expression of the *priA345* mutant is not significantly different from that of the wild type ($P = 0.6$).

[c]Levels of SOS expression were monitored using a *sulAp-gfp* transcriptional reporter inserted into the λ attachment site (32). SOS expression was quantified as the average relative fluorescence intensity (RFI) of pixels for the entire population of cells normalized to the average fluorescence intensity of the background of the images. For each strain, the data were obtained from at least nine different fields taken on three different days. The standard errors of the means for the entire cell population are shown.

[d]Partitioning ability was scored visually by assessing shape of nucleoids across the cell population using a *hupA*::*mCherry* translational fusion reporter (24). Examples of cells that partition their nucleoids similarly to the wild type and those that do not are shown in Fig. 2.

SOS expression, cellular filamentation in the presence of *sulB103* (see below), and defects in chromosome partitioning (reviewed in references 3 and 27). To facilitate this type of phenotypic analysis, we used phase-contrast and fluorescence microscopy on strains that have two types of reporter genes: a *hupA*::*mCherry* translational fusion gene that allows direct visualization of nucleoids without cell fixation or staining to assign a phenotype for nucleoids partitioning (24) and a *sulAp-gfp* transcriptional reporter gene inserted at the λ attachment site to measure SOS expression (31, 32). Neither reporter construct has any negative effect on the cell. All strains also contained a *sulB103* mutation. This is an *ftsZ* allele that is not sensitive to the inhibitory effects of the SOS cell division inhibitor SulA (33). Thus, cellular filamentation (cell area) is an SOS-independent phenotype for these cells.

Single *priA* mutations within the SSB-binding pocket do not perturb cellular phenotypes. The mutations *priA341*(R697A), *priA344*(R697E), and *priA345*(Q701E) in the SSB binding pocket were placed on the chromosome at the native locus for *priA* to facilitate the testing of cellular phenotypes. This was done using recombineering techniques in a "scarless" fashion (see Materials and Methods). The three *priA* mutations were chosen, as follows. *priA341*(R697A) is the mutation evaluated in the smFRET assay *in vitro*. *priA344*(R697E) is a charge reversal mutation of that same residue. It is predicted that the SSB acidic tip would not bind at all due to charge repulsion (21–24) on the acid tip. Finally, *priA345*(Q701E) mutates another residue indicated by the crystallographic studies to have an interaction with the SSB acidic tip (19).

priA-null mutants have severe phenotypes. They grow poorly (34, 35) and are Rec$^-$ (36, 37), sensitive to UV irradiation (UV^s) (34), and sensitive to rich media (38). They also have high basal levels of SOS expression (35) and defects in nucleoid partitioning (31; reviewed in reference 27) and are filamentous even in the presence of a *sulB103* mutation (31). If recruitment by SSB and its remodeling are essential for PriA function in replication restart, then it is predicted that all of these mutants would have phenotypes like that of a *priA*-null mutant. Table 1 and Fig. 2 show that all three mutant strains behave like the *priA*$^+$ strain with regard to the phenotypes of average cell area, basal levels of SOS expression, and chromosome partitioning. The three mutant strains grew well in both minimal and rich media, were resistant to UV irradiation, and were recombination proficient (qualitative patch tests [data not shown]). We conclude that these three *priA* mutations within the SSB-binding pocket do not perturb PriA function in an otherwise wild-type cell.

***priA341*, *priA344*, and *priA345* alleles create modest phenotypes in a *priB*-null strain.** As mentioned above, there are three pathways of replication restart. The PriA-PriB and PriA-PriC pathways are efficient and redundant under most conditions (reviewed in reference 27). The PriC pathway, however, is not very efficient, as seen by

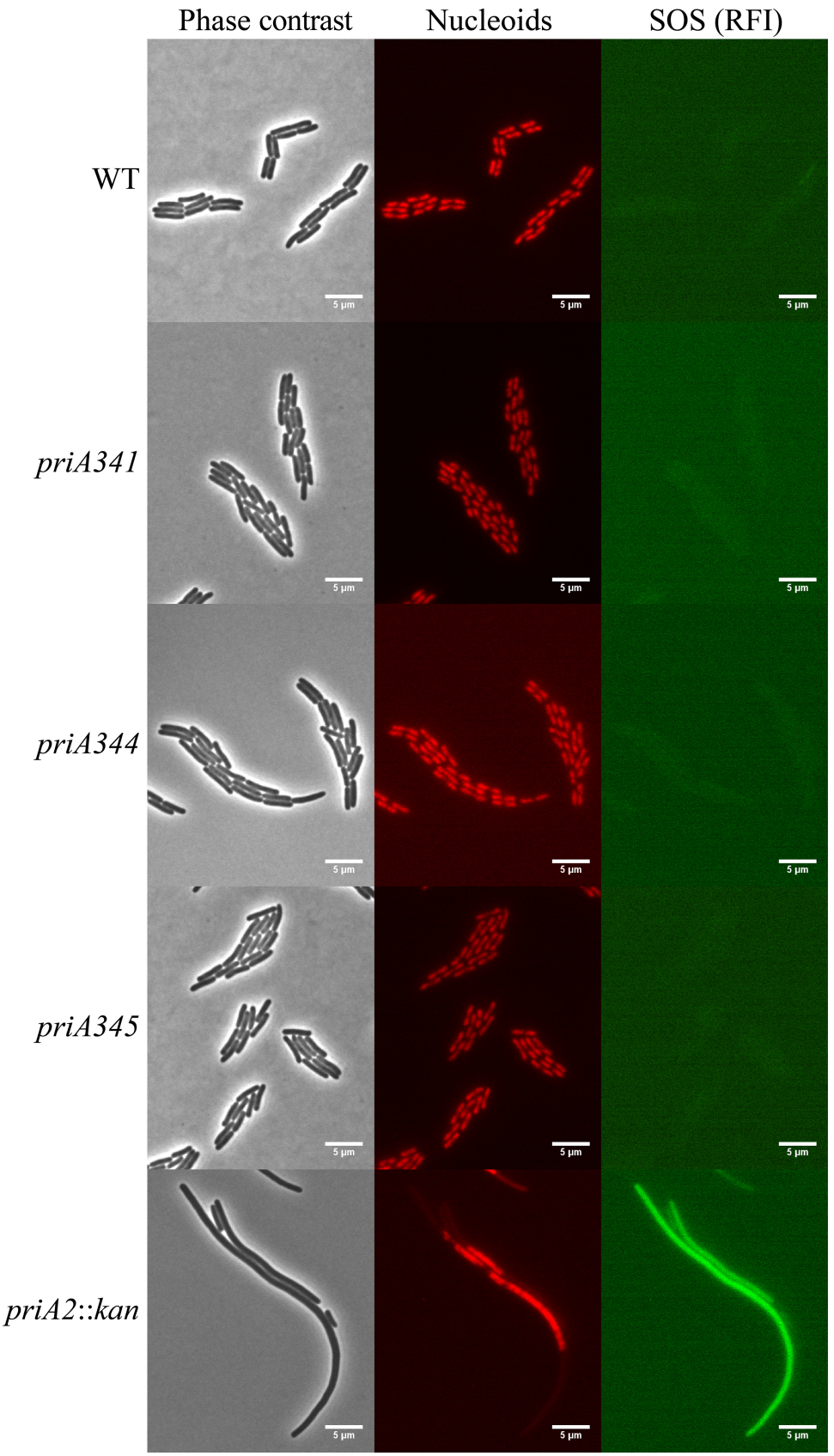

FIG 2 The mutations R697A, R697E, and Q701E in the SSB-binding pocket of *priA* do not cause any significant changes in the cell phenotype. The log-phase cells were grown on minimal medium in slabs of 2% low-melting-

(Continued on next page)

TABLE 2 Effects of *priA* mutations on cell area and level of SOS expression in the Δ*priB* and Δ*priC* strains

Strain	*priA*	*priB*	*priC*	Avg cell area (pixels)[a,b]	SOS (RFI)[b,c]	Partitioning ability[d]	Cell count
SS6321	+	+	+	572 ± 6	2.23 ± 0.04	++	758
SS9116	+	Δ*priB302*	+	584 ± 7	2.42 ± 0.09	++	777
SS11233	+	+	Δ*priC307*	575 ± 6	2.13 ± 0.04	++	1,023
SS11228	*priA341*	+	+	548 ± 5	2.45 ± 0.07	++	1,103
SS11230	*priA341*	Δ*priB302*	+	846 ± 31	4.33 ± 0.21	+	490
SS11232	*priA341*	+	Δ*priC307*	573 ± 5	2.38 ± 0.04	++	1,246
SS11245	*priA344*	+	+	644 ± 7	2.50 ± 0.08	++	1,005
SS11255	*priA344*	Δ*priB302*	+	2,418 ± 139	7.81 ± 0.34	−	500
SS11253	*priA344*	+	Δ*priC307*	700 ± 25	2.30 ± 0.03	++	691
SS11244	*priA345*	+	+	567 ± 5	2.26 ± 0.04	++	1,274
SS11251	*priA345*	Δ*priB302*	+	730 ± 22	3.28 ± 0.10	+	715
SS11249	*priA345*	+	Δ*priC307*	535 ± 5	1.95 ± 0.01	++	1,270

[a]Cells were grown as described in Materials and Methods. One pixel is equal to 0.0625 μm according to our microscopic parameters. The standard errors of the means for the entire cell population are shown.

[b]The average cell areas and levels of SOS expression of the *priA341* Δ*priB302* (SS11230), *priA344* Δ*priB302* (SS11255) and *priA345* Δ*priB302* (SS11251) double mutants are significantly different ($P < 0.001$) from those of the *priA* single mutants (SS11228, SS11245, and SS11244, respectively) and the Δ*priB302* single mutant (SS9116) ($P < 0.001$) by Student's *t* test.

[c]Levels of SOS expression were monitored using a *sulAp-gfp* transcriptional reporter inserted into the λ attachment site (32). SOS expression was quantified as the average relative fluorescence intensity (RFI) of pixels for the entire population of cells normalized to the average fluorescence intensity of the background of the images. For each strain, the data were obtained from at least nine different fields taken on three different days. The standard errors of the means for the entire cell population are shown.

[d]Partitioning ability was scored visually by assessing the shape of nucleoids across the cell population using a *hupA*::*mCherry* translational fusion reporter (24). Examples of cells that partition their nucleoids similarly to the wild type and those that do not are shown in Fig. 2.

the many phenotypes associated with a *priA2*::*kan* mutant. It was shown previously that some *priA* mutations [e.g., *priA300*(K230R) and *priA301*(C479Y)] have no or few phenotypes in an otherwise wild-type cell but do have *priA2*::*kan* null mutant phenotypes if they are combined with a Δ*priB* mutation (39). The simplest explanation for this is that these *priA* mutations remove functions that are required only for the PriA-PriC pathway (and not the PriA-PriB pathway). For this reason, we tested whether the addition of Δ*priB302* would lead to measurable phenotypes for the *priA341*(R697A), *priA344*(R697E), and *priA345*(Q701E) mutant strains. This was done by introducing Δ*priB302* with an appropriately placed Tn*10* marker into strains with the *priA* mutations. Tetracycline-resistant transductants were selected and then screened by PCR for the presence of the deletion. Table 2 shows that in the Δ*priB302* strain, all three *priA* mutants had decreased abilities to perform PriA functions. *priA344*(R697E) showed the largest defect in partitioning ability and the largest increases in average cell area (4-fold) and basal levels of SOS expression (3-fold) of the three mutants. The increases in average cell area and basal levels of SOS expression were 54% and 77%, respectively, for *priA341*(R697A) and 29% and 45%, respectively, for *priA345*(Q701E). In a similar way, the Δ*priC307* mutation was introduced into the three *priA* mutant strains to test if any of the *priA* mutations affected only the PriA-PriB pathway. Table 2 shows also that combination of any of the three *priA* alleles with the Δ*priC307* mutation led to no change in the phenotype relative to the wild type. We conclude that *priA341*(R697A), *priA344*(R697E), and *priA345*(Q701E) affect some activity of PriA necessary in the PriA-PriC pathway but not in the PriA-PriB pathway.

SSB overproduction partially suppresses some phenotypes associated with *priA341*, *priA344*, and *priA345* mutations in the Δ*priB302* strain. To better understand the nature of the defect in the *priA priB* strains presented in Table 2, we wanted to test if we could create conditions that would suppress the phenotypes of the *priA*

FIG 2 Legend (Continued)
point agarose at 37°C for 3 to 4 h before imaging. All strains have a *sulAp-gfp* transcriptional reporter for the SOS response and a *hupA*::*mCherry* translational fusion reporter showing the position of the nucleoids. The three images in each panel are a phase-contrast micrograph and images of nucleoids (red) and SOS (green). Different rows show results for different strains and genotypes: SS6321 (WT), SS11228 (*priA341*), SS11245 (*priA344*), SS11244 (*priA345*), and SS7064 (*priA2*::*kan*). Total magnification, ×1,000.

TABLE 3 Effect of SSB overproduction on the *priA* mutants in the Δ*priB302* background

Strain	*priA*	*priB*	*ssb*	Avg cell area (pixels)[a,b]	SOS (RFI)[b,c]	Partitioning ability[d]	Cell count
SS6321	+	+	+	572 ± 6	2.23 ± 0.04	++	758
SS11234	+	+	*ssbop*	576 ± 5	2.18 ± 0.02	++	1,381
SS9116	+	Δ*priB302*	+	584 ± 7	2.42 ± 0.09	++	777
SS11236	+	Δ*priB302*	*ssbop*	658 ± 7	2.24 ± 0.02	++	983
SS11228	*priA341*	+	+	548 ± 5	2.45 ± 0.07	++	1,103
SS11235	*priA341*	+	*ssbop*	557 ± 5	2.08 ± 0.01	++	1,328
SS11230	*priA341*	Δ*priB302*	+	846 ± 31	4.33 ± 0.21	+	490
SS11237	*priA341*	Δ*priB302*	*ssbop*	940 ± 24	2.42 ± 0.05	+	1,358
SS11245	*priA344*	+	+	644 ± 7	2.50 ± 0.08	++	1,005
SS13467	*priA344*	+	*ssbop*	595 ± 5	2.73 ± 0.04	++	1,298
SS11255	*priA344*	Δ*priB302*	+	2,418 ± 139	7.81 ± 0.34	−	500
SS13468	*priA344*	Δ*priB302*	*ssbop*	902 ± 21	4.49 ± 0.10	+	1,389
SS11244	*priA345*	+	+	567 ± 5	2.26 ± 0.04	++	1,274
SS11256	*priA345*	+	*ssbop*	521 ± 4	2.48 ± 0.06	++	1,648
SS11251	*priA345*	Δ*priB302*	+	730 ± 22	3.28 ± 0.10	+	715
SS11257	*priA345*	Δ*priB302*	*ssbop*	719 ± 17	4.68 ± 0.18	+	1,312

[a]Cells were grown as described in Materials and Methods. One pixel is equal to 0.0625 μm according to our microscopic parameters. The standard errors of the means for the entire cell population are shown.

[b]Statistical analysis was done using Student's *t* test. The average cell area of the *priA341* Δ*priB302 ssbop* (SS11237) triple mutant is not significantly different from that of the *priA341* Δ*priB302* (SS11230) double mutant ($P = 0.03$). The levels of SOS expression between SS11237 and SS11230 differ significantly ($P < 0.001$). The differences in the average cell area and level of SOS expression between the *priA344* Δ*priB302 ssbop* (SS13468) triple mutant and the *priA344* Δ*priB302* (SS11255) double mutant are significant ($P < 0.001$). The average cell area of the *priA345* Δ*priB302 ssbop* triple mutant (SS11257) is not significantly different ($P = 0.7$) from the average cell area of the *priA345* Δ*priB302* double mutant (SS11251). The difference in levels of SOS expression between SS11257 and SS11251 is significant ($P < 0.001$).

[c]Levels of SOS expression were monitored using a *sulAp-gfp* transcriptional reporter inserted into the λ attachment site (32). SOS expression was quantified as the average relative fluorescence intensity (RFI) of pixels for the entire population of cells normalized to the average fluorescence intensity of the background of the images. For each strain, the data were obtained from at least nine different fields taken on three different days. The standard errors of the means for the entire cell population are shown.

[d]Partitioning ability was scored visually by assessing shape of nucleoids across the cell population using a *hupA::mCherry* translational fusion reporter (24). Examples of cells that partition their nucleoids similarly to the wild type and those that do not are shown in Fig. 2.

priB mutants. Two lines of thinking suggested that overproduction of SSB might be able to do this. The first is that PriB and SSB share sequence similarity and an oligonucleotide/oligosaccharide ssDNA-binding fold (40, 41) and that phylogenetic data suggest that a *priB* gene arose as a result of a an *ssb* gene duplication event (42). The second is that it is possible that the *priA* mutations merely decreased the ability of SSB to bind PriA instead of eliminating its ability to bind completely. Therefore, increasing the concentration of SSB might push the equilibrium in favor of binding. In general, however, SSB overproduction could have negative effects on the cell (43, 44).

To overproduce SSB, we introduced a strong constitutive promoter and an improved ribosome binding site (RBS) upstream of the *ssb* gene as previously described for *radA* and *recN* (45, 46). Briefly, the strong promoter and optimized RBS were linked to a flippable chloramphenicol resistance gene and inserted just upstream of the *ssb* gene (see Materials and Methods). This construct was called *ssbop*. The *priA341* Δ*priB302 ssbop*, *priA344* Δ*priB302 ssbop*, and *priA345* Δ*priB302 ssbop* triple mutants were constructed in a two-step process. First, *ssbop* was transduced into the *priA341*, *priA344*, and *priA345* single mutant strains by selecting for chloramphenicol resistance, and then the Δ*priB302* mutation was introduced with tetracycline resistance. Table 3 shows that *ssbop* positively impacted two *priA priB* double mutants and negatively impacted the third. The largest positive effect was seen with the *priA344* Δ*priB302* double mutant. Here, all of the phenotypes improved: the defect of nucleoid partitioning was less apparent, the cells had a smaller average cell area (3-fold) and the levels of SOS expression were 2-fold less. Overproduction of SSB rescued only the high SOS expression of the *priA341* Δ*priB302* double mutant (a change in relative fluorescence intensity [RFI] from 4.33 to 2.42). There was no significant effect on the average cell area. *ssbop* failed to suppress any of the phenotypes of the *priA345* Δ*priB302* mutation. In fact, the presence of *ssbop* increased the SOS levels by 30%. Table 3 also shows that for the phenotypes tested here, *ssbop* had no negative impact on the cell even though

TABLE 4 Phenotypic characterization of the *priC351* mutation within the SSB-binding pocket

Strain	*priA*	*priB*	*priC*	Avg cell area (pixels)[a,b]	SOS (RFI)[b,c]	Cell area < 300		Cell area > 300		Partitioning ability[d]	Cell count
						SOS (RFI)	% population	SOS (RFI)	% population		
SS6321	+	+	+	184 ± 1	3.1 ± 0.1	2.9	98	9.3	2	++	6,489
SS12997	+	+	*priC351*	197 ± 1	4.4 ± 0.1	4.0	96	12.1	4	++	2,829
SS9114	+	+	*priC303*::*kan*	193 ± 1	2.8 ± 0.1	2.7	96	4.6	4	++	2,265
SS9116	+	Δ*priB302*	+	187 ± 2	4.7 ± 0.2	4.3	96	15.8	4	++	1,654
SS13407	+	Δ*priB302*	*priC351*	806 ± 39	22.7 ± 0.7	17.2	56	29.8	44	−	1,404
SS13420	+	Δ*priB302*	*priC303*::*kan*	538 ± 34	13.6 ± 0.6	10.3	64	19.4	36	−	1,347
SS7064	*priA2*::*kan*	+	+	675 ± 24	24.5 ± 1.0	16.8	46	31.0	54	−	988

[a]Cells were grown as described in Materials and Methods. One pixel is equal to 0.1073 μm according to our microscopic parameters. The standard errors of the means for the entire cell population are shown.

[b]Statistical analysis was done using Student's *t* test. The average cell area of the *priC351* (SS12997) was not statistically significantly different from the average cell area of the *priC303*::*kan* (SS9114) mutant ($P = 0.03$). The difference in levels of the SOS expression between SS12997 and SS9114 is significant ($P < 0.001$). The average cell area and level of SOS expression of the Δ*priB302 priC351* (SS13407), Δ*priB302 priC303*::*kan* (SS13420), and *priA2*::*kan* (SS7064) mutants are significantly different ($P < 0.001$) from those of the wild type (SS6321).

[c]Levels of SOS expression were monitored using a *sulAp-gfp* transcriptional reporter inserted into the λ attachment site (32). SOS expression was quantified as average relative fluorescence intensity (RFI) of pixels for the entire population of cells normalized to the average fluorescence intensity of the background of the images. For each strain, the data were obtained from at least nine different fields taken on three different days. The standard errors of the means for the entire cell population are shown.

[d]Partitioning ability was scored visually by assessing shape of nucleoids across the cell population using a *hupA*::*mCherry* translational fusion reporter (24). Examples of cells that partition their nucleoids similarly to the wild type and those that do not are shown in Fig. 2.

overproduction of SSB from a plasmid has been shown to negatively impact cellular function related to SOS induction and recombination (43, 44). We conclude that overproduction of SSB is able to suppress some of the negative phenotypes of the *priA341* Δ*priB302* and *priA344* Δ*priB302* double mutants but not of the *priA345* Δ*priB302* mutant.

A strain with *priC351*(R155A) on the chromosome acts like a *priC*-null mutant *in vivo*. *priC351*(R155A) was not able to complement *priC303*::*kan* in a plasmid-based assay *in vivo* (30). We wanted to measure *priC351*'s phenotypes when it was expressed from its native locus on the chromosome. To do this, we first placed this mutation on the chromosome using recombineering techniques as described in Materials and Methods. We then characterized the phenotypes of *priC351*(R155A) by standard phase-contrast and fluorescence microscopy. Table 4 shows that the single *priC351*(R155A) mutant behaved as the wild type for the phenotypes tested.

The above result was expected, as *priB* and *priC* have redundant functions (47). Initial characterization of the Δ*priB302 priC303*::*kan* double mutant showed that it grew very poorly, even more poorly than a *priA2*::*kan* mutant (47). The small colonies that did grow often acquired suppressor mutations (47). Here, we report how we could construct and grow these very poorly growing mutants reproducibly so that we could further characterize them. To do this, we transduced the Δ*priB302* mutation into the *priC* mutant, incubating the transductant on minimal medium plates at 37°C for 3 to 4 days. Very small transductants were formed. These transductants were then subjected to 2 rounds of colony purification (incubated for 48 h each on minimal medium). By purifying the small colonies each time, we were able to consistently get small colonies without too many large ones. Individual small colonies were then used to make patches on minimal medium plates that could then be used to reproducibly inoculate and grow cultures. Since these strains grew very slowly and there was a high probability of suppressors arising in the population, we tested our cultures at the end of all experiments by streaking cells on minimal medium plates to be sure that only the small-colony phenotype was seen and no suppressors (large colonies) arose in that culture.

Table 4 shows the results of the microscopic characterization of the *priBC* double mutants. These cells were imaged at a magnification of ×600 instead of ×1,000, the magnification used for the strains characterized in Tables 1 to 3. Hence, the average cell area and levels of SOS expression are not directly comparable between tables. Microscopic analysis of cultures of Δ*priB302 priC351*(R155A) and Δ*priB302 priC303*::*kan* cells grown in minimal medium showed that the populations of cells were composed of both wild-type-looking and filamentous cells (Fig. 3). Table 4 shows that in general,

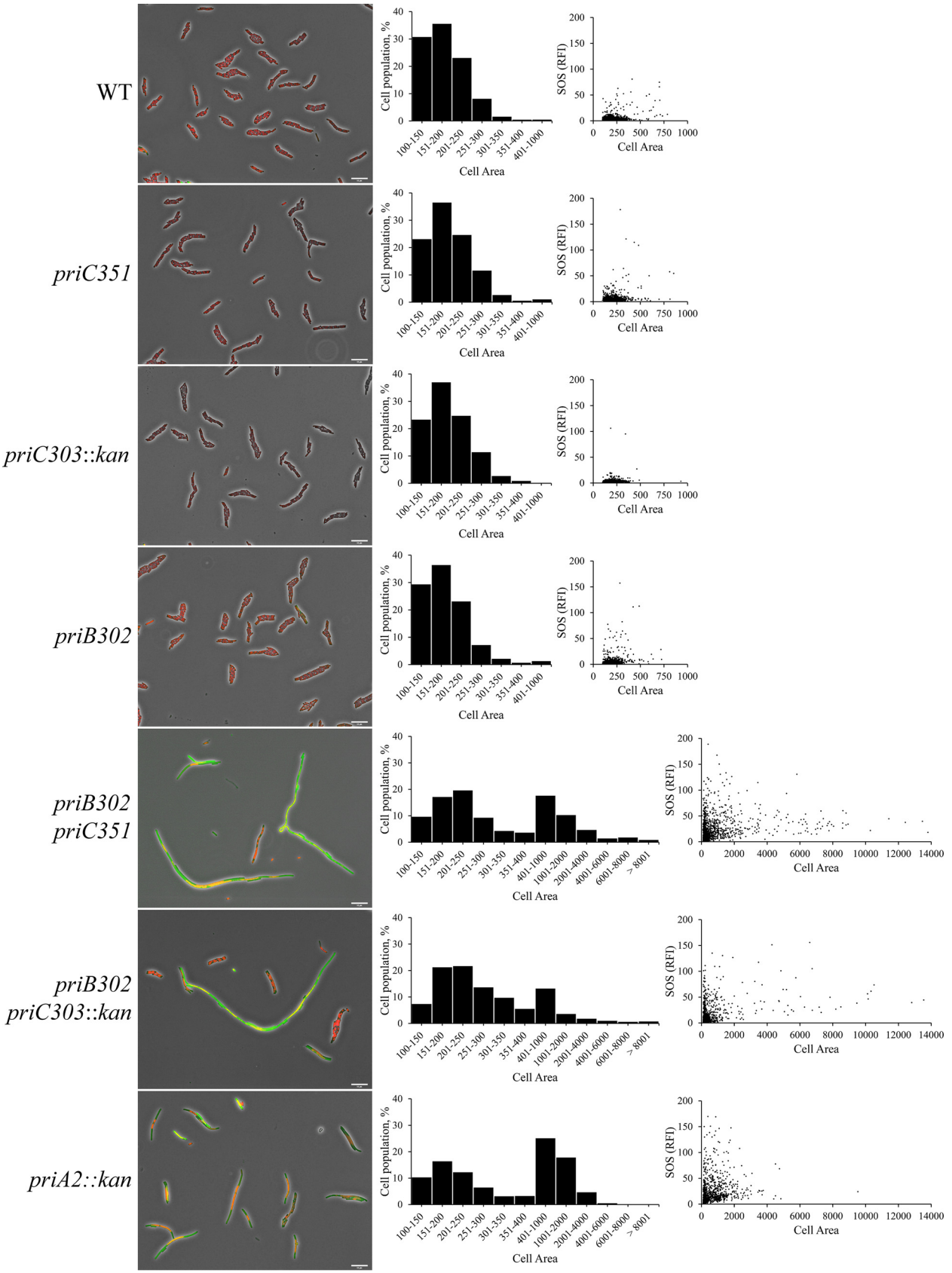

FIG 3 Phenotypes of the Δ*priB302 priC351* and Δ*priB302 priC303*::*kan* double mutants. (Left) The mutation R155A in the SSB-binding pocket of *priC* does not have any noticeable phenotype by itself compared to the wild-type strain. In contrast, both Δ*priB302 priC351* and Δ*priB302 priC303*::*kan*

(Continued on next page)

Δ*priB302 priC351*(R155A) and Δ*priB302 priC303*::*kan* mutants were similar to the *priA2*::*kan* mutants. They showed 3- to 4-fold increases in average cell area and 3- to 5-fold increases in SOS expression, with the Δ*priB302 priC351* mutant showing greater increases than the Δ*priB302 priC303*::*kan* mutant for both phenotypes. Both strains showed the partitioning defect. Binning of the data into two groups based on cell area (less than or equal to 300 pixels in cell area with cells that are greater than 300 pixels) showed that between 36 and 44% of the cells were filamentous. The level of SOS expression in the filamentous cells with areas greater than 300 pixels were about 2-fold higher on average than the level in cells with areas less than or equal to 300 pixels (Fig. 3 and Table 4). Both groups had higher values than the wild type or either single mutant in both categories. The data support the previous findings that *priC351*(R155A) does not complement a *priC303*::*kan* mutation and show that this mutation tends to produce slightly more detrimental phenotypes than the *priC303*::*kan* mutation. It is also seen that the *priBC* double mutants have phenotypes similar to that of a *priA* null mutant, with two distinct populations of cells (normal-length and highly filamentous cells), high basal levels of SOS expression, and defects in nucleoid partitioning.

DISCUSSION

In vitro, the replication restart proteins PriA and PriC have been shown to interact with SSB through the C-terminal acidic tip (19, 20) and remodel the conformation of the SSB on ssDNA from an SSB_{65} mode to a SSB_{35} mode (9, 10; reviewed in references 4 and 5). This work included the identification of certain residues in PriA and PriC that were required for the *in vitro* reactions (19, 20). It has been hypothesized that the *in vivo* importance of these reactions is that a region of ssDNA is liberated so that DnaC can load DnaB onto the lagging strand template during replication restart. Only the PriC mutants were shown not to be able to complement a chromosomal null mutation expressed from a plasmid (20). At the time of the previous publications, the identified residues in the PriA's SSB-binding pocket had not been tested for complementation *in vivo* (19). Thus, this work continued those studies and tested the importance of the PriA and PriC residues *in vivo* by first placing them on the chromosome and then characterizing them using standard assays for replication restart mutants. As expected, the mutations in PriC that destroyed the ability to interact with SSB and remodel the SSB on ssDNA *in vitro* effectively result in a null mutant phenotype *in vivo*. Unexpectedly, however, we found that the three mutations tested in the PriA SSB-binding pocket did not cause a null mutant phenotype as single mutations in an otherwise wild-type cell. This was unexpected because they had the same effects as mutations in the SSB-binding site of PriC on the assay *in vitro* and it was assumed, supported by experiments and rationale mentioned above, that the SSB-PriA interactions would be important for PriA's function *in vivo*.

The removal of PriB unmasked a requirement for the SSB-binding pocket in the PriA-PriC pathway for the three *priA* mutant strains. This too was unexpected, because PriC, as well as PriA, can interact with SSB and remodel it, as shown *in vitro*. This prompts the questions of why the PriA SSB-binding pocket is required only in the PriA-PriC pathway (and not the PriA-PriB pathway) and why the PriC SSB-binding pocket is not sufficient *in vivo* in the *priB* mutant. While the answers to these questions are not clear, one possibility is that the interaction of PriA with SSB in replication restart is required before PriC is loaded. Another is that the SSB tetramer forms a bridge between the PriA and PriC proteins via two of the acidic tips.

FIG 3 Legend (Continued)
double mutants show many filamentous cells that are highly induced for SOS and have poorly partitioned nucleoids. Overnight cultures were grown on minimal medium in slabs of 2% low-melting-point agarose at 37°C for 3 to 4 h before imaging. All strains have a *sulAp-gfp* transcriptional reporter for the SOS response and a *hupA*::*mCherry* translational fusion reporter showing the position of nucleoids. The images are overlays of a phase-contrast image and images showing nucleoids (red) and SOS (green). Bars, 10 μm. Total magnification, ×600. (Middle) Binning of the cell area from 100 pixels (lowest) to 14,000 pixels (highest), with 50-pixel increments. The population of cells representing less than 1% was combined in one column (15th through 548th increments). (Right) Distribution of individual cells in the entire population by cell area and RFI (SOS). Different rows show results for different strains and genotypes: SS6321 (WT), SS12997 (*priC351*), SS9114 (*priC303*::*kan*), SS9116 (Δ*priB302*), SS13407 (Δ*priB302 priC351*), SS13420 (Δ*priB302 priC303*::*kan*) and SS7064 (*priA2*::*kan*).

Another unexpected observation was that overproduction of SSB was able to suppress some of the phenotypes of some of the *priA* single mutants in the Δ*priB* strain. The fact that more suppression was seen with some mutations than others suggests that the mode of suppression is not a new general indirect pathway (like *dnaC809* suppression of *priA*-null mutations [37]) but is instead some sort of direct interaction. It is possible that the mutations decrease the ability of PriA to bind SSB to different degrees, and then the increased concentration of SSB is able to overcome this decreased interaction to various degrees by mass action. An alternative explanation for the SSB suppression in the absence of PriB could be that PriB and SSB have similar structures and that increased amounts of SSB are somehow able to partially substitute for PriB in this situation.

This is the first study in which *priBC* double mutants have been characterized in more depth other than showing a severe qualitative growth defect relative to either of the two single mutations or the *priA2*::*kan* mutation (47). The nucleoid partitioning ability, the two distinct subpopulations of cells, and the high basal levels of SOS expression are highly reminiscent of *priA*-null mutants (31). It should be remembered, however, that a distinguishing characteristic of the *priBC* mutants, versus the *priA*-null mutants, is that they take a much longer time for colony formation.

Given the current model of *E. coli* having three pathways and the assumption that replication restart is essential for cell viability, one must rationalize the marginal viability of *priBC* mutants. One simple idea is suggested by the two populations seen in the microscopic images of *priBC* mutants that contain both wild-type-looking cells and filamentous cells with Par$^-$ nucleoids. This suggests that when a replication fork breaks and is repaired, it cannot simply be restarted because all three pathways of restart are inactivated. What then happens to this repaired fork is critical for the phenotype seen. It is possible that the newly synthesized arms of the replicating chromosome are degraded so that a single circular chromosome remains and it can begin replication again at *oriC* (48–50). This cell would likely be similar in size to a normal cell with a single nucleoid and might show higher-than-normal levels of SOS expression (these types of cells are seen [Fig. 3]). Alternatively, the abandoned repaired fork is likely still a substrate for the DNA replication and recombination machineries. Its further processing does not, however, yield a whole chromosome that can be segregated to a daughter cell. Instead, it produces a contiguous mass of DNA along the length of the filamentous cell. This process might be similar to late DNA replication of bacteriophage T4, where recombination primes DNA replication to make branched structures (51). This model is supported by the observation that the Par$^-$ phenotype in a *priA2*::*kan* mutant is largely suppressed by removing the recombination machinery (31). These *priA recA* cells have reasonably partitioned nucleoids but still filament and grow poorly. They can, however, restart forks because of the presence of the PriC pathway. The marginal viability of *priBC* mutants is then seen as the low probability that the chromosome can be replicated without suffering an insult that requires restart. While models predict that this would be infrequent, it could happen just often enough to explain the very slow growth of the *priBC* colony or culture when the most favorable of conditions are used.

Finally, it is worth emphasizing that the ability to control and modulate SSB binding and ssDNA during replication restart must be extremely important, as the cell has evolved three separate mechanisms to do this for the three different pathways of replication restart. For the PriA-PriB, PriA-PriC, and PriC pathways, these are the PriA-PriB interaction presumably through the cysteine-rich region (52) (remembering that SSB and PriB both bind ssDNA and share structure and evolutionary history [see above]), the PriA-SSB interaction through the SSB binding pocket, and PriC-SSB interaction, respectively.

MATERIALS AND METHODS

Strains, media, and other reagents. All bacterial strains are derivatives of *Escherichia coli* K-12 and are characterized in Table S1 in the supplemental material. The strains were generated using either linear transformation or P1 transduction according to previously described protocols (53, 54). Transformants and transductants were selected on 2% agar plates containing either Luria broth or 56/2 minimal

medium supplemented with 0.2% glucose, 0.001% thiamine, 0.02% arginine, 0.005% histidine, 0.02% proline, and appropriate antibiotics (53). Ampicillin was used at 50 μg/ml, anhydrotetracycline hydrochloride at 5 μg/ml, chloramphenicol at 25 μg/ml, kanamycin at 50 μg/ml, and tetracycline at 10 μg/ml. The cells were purified on the same type of medium on which they were selected and grown at 30°C or 37°C. L-Arabinose was used for induction of the λ Red expression plasmid pKD46 at a final concentration of 0.5% (wt/vol). All plasmids and oligonucleotide primers used in this work are described in Tables S1 and S2, respectively.

Mutagenesis of the *priA* gene. Mutations in the *priA* gene, *priA341*(R697A), *priA344*(R697E), and *priA345*(Q701E), were introduced via scarless site-directed mutagenesis using a method described by Blank and colleagues (55). The method involves the combination of the Red recombinase system of phage λ and counterselection with the help of I-SceI endonuclease introducing double-strand breaks in DNA of the unsuccessful recombinants. Oligonucleotide primers prSJS1511 and prSJS1512 (Table S2) were used to amplify an I-SceI recognition site and a chloramphenicol resistance cassette between two Flp recombination target (FRT) sites (I-SceI *FRTcat*) from pWRG100 template plasmid. These primers contained 40-bp extensions at the 5′ ends homologous to regions immediately upstream and downstream of a codon of the *priA* gene encoding the R697 residue. After amplification, a 1,080-bp PCR product was integrated within the *priA* gene on the chromosome by linear transformation into SS11301 strain using standard recombineering methods (54). Transformants were selected for chloramphenicol resistance on rich medium at 37°C. The proper insertion of the cassette was verified by PCR with prSJS1511 and prSJS1512. The mutant cells were cured of pKD46 and tested for ampicillin sensitivity. The resulting strain was designated SS11225. This strain was then chemically transformed with pWRG99 and selected for ampicillin resistance on rich medium at 30°C to give SS11226.

Pairs of 70-mer or 80-mer DNA oligonucleotides were designed for site-directed mutagenesis of the *priA* gene: prSJS1498 and prSJS1513 for *priA341*, prSJS1560 and prSJS1561 for *priA344*, and prSJS1558 and prSJS1559 for *priA345*. These oligonucleotides contain mutated *priA* alleles in the central part flanked by the homologous sequences used for integration of the I-SceI *FRTcat* cassette. In addition, the *priA341* and *priA345* alleles contain a novel BsiWI restriction site introduced at V698 to facilitate initial screening of mutants via restriction fragment length polymorphism analysis. For each pair, oligonucleotides were hybridized to form DNA duplexes. These duplexes were then transformed into electrocompetent SS11226 cells and integrated within the *priA* gene to replace the I-SceI *FRTcat* cassette using λ Red recombinase genes expressed from pWRG99 plasmid (55). Transformants were selected for ampicillin resistance on rich medium containing 5 μg/ml of anhydrotetracycline hydrochloride at 30°C and screened for chloramphenicol sensitivity. Successful recombinants were verified by PCR of genomic DNA with prSJS1235 and prSJS1330 followed by digestion with BsiWI (if applicable) and finally by DNA sequencing with prSJS1235, prSJS1237, and prSJS1330. The strains harboring the *priA341*, *priA344*, and *priA345* alleles were designated SS11227, SS11241, and SS11242, respectively. The cells were cured of pWRG99 by P1 transduction of the mutations into SS11217 to create SS11228 (*priA341*), SS11245 (*priA344*), and SS11244 (*priA345*).

Mutagenesis of the *priC* gene. *priC351*(R155A) was introduced in the *priC* gene using a method similar to the one applied for an insertion of the I-SceI *FRTcat* cassette into the *priA* gene. Oligonucleotide primers prSJS1638 and prSJS594 were used to amplify a mutated *priC* allele and a kanamycin resistance cassette from SS4395. prSJS1638 was designed with homology to the *priC* gene and contains a *priC351* allele in its second half and a novel Sau96I site to facilitate screening. A 1,537-bp PCR fragment was used to transform electrocompetent SS11301 cells using standard recombineering methods (54). Transformants were selected for kanamycin resistance on minimal medium at 37°C. A construct with *priC351*(R155A) was verified by PCR analysis with prSJS626 and prSJS625. The kanamycin resistance marker was removed from the chromosome by Flp-mediated recombination using plasmid pCP20 (56) to give strain SS12677. The presence of the *priC351* mutation was confirmed by DNA sequencing with prSJS718 and prSJS594. *ybaM*$^+$ was then reintroduced on the chromosome next to *priC351* using a flippable chloramphenicol resistance cassette and a method similar to the one described above. Briefly, a *ybaM*$^+$ *FRTcat* fragment (1,218 bp) was generated in a crossover PCR with a *ybaM* gene amplified from strain JC13509 with prSJS1694 and prSJS1696 and the chloramphenicol resistance cassette amplified from the (*cat*) *recNop* construct (45) with prSJS1695 and prSJS1697. This fragment was transformed into electrocompetent SS12977 cells and placed downstream of the *priC351*(R155A) mutation using standard recombineering methods (54). The chloramphenicol resistance marker was removed using Flp-mediated recombination as previously described (56) to give strain SS12997. The construct was confirmed by DNA sequencing with prSJS718 and prSJS608.

Microscopy and image analysis. Cells were grown overnight in 56/2 minimal medium. Then, 175 μl of the culture was added to 3 ml of 56/2 minimal medium and grown for 3 h to early log phase. Three microliters of the log-phase or overnight culture was loaded onto a 2% agarose slab prepared from 56/2 minimal medium and low-melting-point agarose. A coverslip was mounted on top, and the slides were incubated for 3 to 4 h at 37°C. Cells were visualized using a Nikon E600 microscope equipped with automated filter wheels, shutters, a CoolLED light source, and an ORCA-ER camera. Phase-contrast and fluorescent images were taken for at least 9 different fields of view (3 fields on 3 different days). These images were analyzed with the following software: I-Vision (BioVision Technologies, Inc.), OpenLabs 5.5.1 (Improvision, Inc.), Oufti (57), SuperSegger (58), and MatLab R2016a and R2019a (MathWorks, Inc.). Individual cells were outlined using Oufti or SuperSegger. Strains were analyzed for number of cells, cell area, and intensity of the fluorescent signal using specially written Matlab programs. Statistical analysis of data was performed using Student's *t* test. A cutoff *P* value of <0.001 was used to determine significance. *P* values are reported in the footnotes for each table. The cell area is given as a total number

of pixels in a cell, where one pixel is equal to 0.0625 μm at a $\times$1,000 total magnification and 0.1073 μm at a $\times$600 total magnification.

SUPPLEMENTAL MATERIAL

Supplemental material is available online only.

SUPPLEMENTAL FILE 1, PDF file, 0.3 MB.

ACKNOWLEDGMENTS

This work was supported by R01 GM098885 from the National Institutes of Health.

We thank Roman G. Gerlach for sending plasmids pWRG99 and pWRG100. We also thank James L. Keck for reading the manuscript before publication and offering suggestions.

REFERENCES

1. Cox MM, Goodman MF, Kreuzer KN, Sherratt DJ, Sandler SJ, Marians KJ. 2000. The importance of repairing stalled replication forks. Nature 404:37–41. https://doi.org/10.1038/35003501.
2. Michel B, Sinha AK, Leach DRF. 2018. Replication fork breakage and restart in *Escherichia coli*. Microbiol Mol Biol Rev 82:e00013-18. https://doi.org/10.1128/MMBR.00013-18.
3. Windgassen TA, Wessel SR, Bhattacharyya B, Keck JL. 2018. Mechanisms of bacterial DNA replication restart. Nucleic Acids Res 46:504–519. https://doi.org/10.1093/nar/gkx1203.
4. Shereda RD, Kozlov AG, Lohman TM, Cox MM, Keck JL. 2008. SSB as an organizer/mobilizer of genome maintenance complexes. Crit Rev Biochem Mol Biol 43:289–318. https://doi.org/10.1080/10409230802341296.
5. Antony E, Lohman TM. 2019. Dynamics of *E. coli* single stranded DNA binding (SSB) protein-DNA complexes. Semin Cell Dev Biol 86:102–111. https://doi.org/10.1016/j.semcdb.2018.03.017.
6. Savvides SN, Raghunathan S, Fütterer K, Kozlov AG, Lohman TM, Waksman G. 2004. The C-terminal domain of full-length *E. coli* SSB is disordered even when bound to DNA. Protein Sci 13:1942–1947. https://doi.org/10.1110/ps.04661904.
7. Shishmarev D, Wang Y, Mason CE, Su X-C, Oakley AJ, Graham B, Huber T, Dixon NE, Otting G. 2014. Intramolecular binding mode of the C-terminus of *Escherichia coli* single-stranded DNA binding protein determined by nuclear magnetic resonance spectroscopy. Nucleic Acids Res 42:2750–2757. https://doi.org/10.1093/nar/gkt1238.
8. Raghunathan S, Ricard CS, Lohman TM, Waksman G. 1997. Crystal structure of the homo-tetrameric DNA binding domain of *Escherichia coli* single-stranded DNA-binding protein determined by multiwavelength X-ray diffraction on the selenomethionyl protein at 2.9-A resolution. Proc Natl Acad Sci U S A 94:6652–6657. https://doi.org/10.1073/pnas.94.13.6652.
9. Lohman TM, Overman LB. 1985. Two binding modes in *Escherichia coli* single strand binding protein-single stranded DNA complexes. Modulation by NaCl concentration. J Biol Chem 260:3594–3603.
10. Bujalowski W, Lohman TM. 1986. *Escherichia coli* single-strand binding protein forms multiple, distinct complexes with single-stranded DNA. Biochemistry 25:7799–7802. https://doi.org/10.1021/bi00372a003.
11. Bujalowski W, Overman LB, Lohman TM. 1988. Binding mode transitions of *Escherichia coli* single strand binding protein-single-stranded DNA complexes. Cation, anion, pH, and binding density effects. J Biol Chem 263:4629–4640.
12. Lohman TM, Overman LB, Datta S. 1986. Salt-dependent changes in the DNA binding co-operativity of *Escherichia coli* single strand binding protein. J Mol Biol 187:603–615. https://doi.org/10.1016/0022-2836(86)90338-4.
13. Overman LB, Lohman TM. 1994. Linkage of pH, anion and cation effects in protein-nucleic acid equilibria. J Mol Biol 236:165–178. https://doi.org/10.1006/jmbi.1994.1126.
14. Lohman TM, Bujalowski W, Overman LB. 1988. *E. coli* single strand binding protein: a new look at helix-destabilizing proteins. Trends Biochem Sci 13:250–255.
15. Lu D, Keck JL. 2008. Structural basis of *Escherichia coli* single-stranded DNA-binding protein stimulation of exonuclease I. Proc Natl Acad Sci U S A 105:9169–9174. https://doi.org/10.1073/pnas.0800741105.
16. Chase JW, L'Italien JJ, Murphy JB, Spicer EK, Williams KR. 1984. Characterization of the *Escherichia coli* SSB-113 mutant single-stranded DNA-binding protein. Cloning of the gene DNA and protein sequence analysis, high pressure liquid chromatography peptide mapping, and DNA-binding studies. J Biol Chem 259:805–814.
17. Curth U, Genschel J, Urbanke C, Greipel J. 1996. *In vitro* and *in vivo* function of the C-terminus of *Escherichia coli* single-stranded DNA binding protein. Nucleic Acids Res 24:2706–2711. https://doi.org/10.1093/nar/24.14.2706.
18. Genschel J, Curth U, Urbanke C. 2000. Interaction of *E. coli*-single-stranded DNA binding protein (SSB) with exonuclease I. The carboxy-terminus of SSB is the recognition site for the nuclease. Biol Chem 381:183–192.
19. Bhattacharyya B, George NP, Thurmes TM, Zhou R, Jani N, Wessel SR, Sandler SJ, Ha T, Keck JL. 2014. Structural mechanisms of PriA-mediated DNA replication restart. Proc Natl Acad Sci U S A 111:1373–1378. https://doi.org/10.1073/pnas.1318001111.
20. Wessel SR, Cornilescu CC, Cornilescu G, Metz A, Leroux M, Hu K, Sandler SJ, Markley JL, Keck JL. 2016. Structure and function of the PriC DNA replication restart protein. J Biol Chem 291:18384–18396. https://doi.org/10.1074/jbc.M116.738781.
21. Ryzhikov M, Koroleva O, Postnov D, Tran A, Korolev S. 2011. Mechanism of RecO recruitment to DNA by single-stranded DNA binding protein. Nucleic Acids Res 39:6305–6314. https://doi.org/10.1093/nar/gkr199.
22. Shereda RD, Reiter NJ, Butcher SE, Keck JL. 2009. Identification of the SSB binding site on *E. coli* RecQ reveals a conserved surface for binding SSB's C terminus. J Mol Biol 386:612–625. https://doi.org/10.1016/j.jmb.2008.12.065.
23. Petzold C, Marceau AH, Miller KH, Marqusee S, Keck JL. 2015. Interaction with single-stranded DNA-binding protein stimulates *Escherichia coli* ribonuclease HI enzymatic activity. J Biol Chem 290:14626–14636. https://doi.org/10.1074/jbc.M115.655134.
24. Marceau AH, Bahng S, Massoni SC, George NP, Sandler SJ, Marians KJ, Keck JL. 2011. Structure of the SSB-DNA polymerase III interface and its role in DNA replication. EMBO J 30:4236–4247. https://doi.org/10.1038/emboj.2011.305.
25. Butland G, Peregrin-Alvarez JM, Li J, Yang W, Yang X, Canadien V, Starostine A, Richards D, Beattie B, Krogan N, Davey M, Parkinson J, Greenblatt J, Emili A. 2005. Interaction network containing conserved and essential protein complexes in *Escherichia coli*. Nature 433:531–537. https://doi.org/10.1038/nature03239.
26. Arifuzzaman M, Maeda M, Itoh A, Nishikata K, Takita C, Saito R, Ara T, Nakahigashi K, Huang H-C, Hirai A, Tsuzuki K, Nakamura S, Altaf-Ul-Amin M, Oshima T, Baba T, Yamamoto N, Kawamura T, Ioka-Nakamichi T, Kitagawa M, Tomita M, Kanaya S, Wada C, Mori H. 2006. Large-scale identification of protein-protein interaction of *Escherichia coli* K-12. Genome Res 16:686–691. https://doi.org/10.1101/gr.4527806.
27. Michel B, Sandler SJ. 2017. Replication restart in bacteria. J Bacteriol 199:e00102-17. https://doi.org/10.1128/JB.00102-17.
28. Cadman CJ, McGlynn P. 2004. PriA helicase and SSB interact physically and functionally. Nucleic Acids Res 32:6378–6387. https://doi.org/10.1093/nar/gkh980.
29. Kozlov AG, Jezewska MJ, Bujalowski W, Lohman TM. 2010. Binding specificity of *E. coli* SSB protein for the χ subunit of DNA pol III holoenzyme and PriA helicase. Biochemistry 49:3555–3566. https://doi.org/10.1021/bi100069s.
30. Wessel SR, Marceau AH, Massoni SC, Zhou R, Ha T, Sandler SJ, Keck JL.

2013. PriC-mediated DNA replication restart requires PriC complex formation with the single-stranded DNA-binding protein. J Biol Chem 288:17569–17578. https://doi.org/10.1074/jbc.M113.478156.
31. McCool JD, Sandler SJ. 2001. Effects of mutations involving cell division, recombination, and chromosome dimer resolution on a *priA2*::*kan* mutant. Proc Natl Acad Sci U S A 98:8203–8210. https://doi.org/10.1073/pnas.121007698.
32. McCool JD, Long E, Petrosino JF, Sandler HA, Rosenberg SM, Sandler SJ. 2004. Measurement of SOS expression in individual *Escherichia coli* K-12 cells using fluorescence microscopy. Mol Microbiol 53:1343–1357. https://doi.org/10.1111/j.1365-2958.2004.04225.x.
33. Bi E, Lutkenhaus J. 1990. Analysis of *ftsZ* mutations that confer resistance to the cell division inhibitor SulA (SfiA). J Bacteriol 172:5602–5609. https://doi.org/10.1128/jb.172.10.5602-5609.1990.
34. Lee EH, Kornberg A. 1991. Replication deficiencies in *priA* mutants of *Escherichia coli* lacking the primosomal replication n′ protein. Proc Natl Acad Sci U S A 88:3029–3032. https://doi.org/10.1073/pnas.88.8.3029.
35. Nurse P, Zavitz KH, Marians KJ. 1991. Inactivation of the *Escherichia coli* PriA DNA replication protein induces the SOS response. J Bacteriol 173:6686–6693. https://doi.org/10.1128/jb.173.21.6686-6693.1991.
36. Kogoma T, Cadwell GW, Barnard KG, Asai T. 1996. The DNA replication priming protein, PriA, is required for homologous recombination and double-strand break repair. J Bacteriol 178:1258–1264. https://doi.org/10.1128/jb.178.5.1258-1264.1996.
37. Sandler SJ, Samra HS, Clark AJ. 1996. Differential suppression of *priA2*::*kan* phenotypes in *Escherichia coli* K-12 by mutations in *priA*, *lexA*, and *dnaC*. Genetics 143:5–13.
38. Masai H, Asai T, Kubota Y, Arai K, Kogoma T. 1994. *Escherichia coli* PriA protein is essential for inducible and constitutive stable DNA replication. EMBO J 13:5338–5345. https://doi.org/10.1002/j.1460-2075.1994.tb06868.x.
39. Sandler SJ, McCool JD, Do TT, Johansen RU. 2001. PriA mutations that affect PriA-PriC function during replication restart. Mol Microbiol 41:697–704. https://doi.org/10.1046/j.1365-2958.2001.02547.x.
40. Lopper M, Boonsombat R, Sandler SJ, Keck JL. 2007. A hand-off mechanism for primosome assembly in replication restart. Mol Cell 26:781–793. https://doi.org/10.1016/j.molcel.2007.05.012.
41. Raghunathan S, Kozlov AG, Lohman TM, Waksman G. 2000. Structure of the DNA binding domain of *E. coli* SSB bound to ssDNA. Nat Struct Biol 7:648–652. https://doi.org/10.1038/77943.
42. Ponomarev VA, Makarova KS, Aravind L, Koonin EV. 2003. Gene duplication with displacement and rearrangement: origin of the bacterial replication protein PriB from the single-stranded DNA-binding protein SSB. J Mol Microbiol Biotechnol 5:225–229. https://doi.org/10.1159/000071074.
43. Moreau PL. 1987. Effects of overproduction of single-stranded DNA-binding protein on RecA protein-dependent processes in *Escherichia coli*. J Mol Biol 194:621–634. https://doi.org/10.1016/0022-2836(87)90239-7.
44. Moreau PL. 1988. Overproduction of single-stranded-DNA-binding protein specifically inhibits recombination of UV-irradiated bacteriophage DNA in *Escherichia coli*. J Bacteriol 170:2493–2500. https://doi.org/10.1128/jb.170.6.2493-2500.1988.
45. Warr AR, Klimova AN, Nwaobasi AN, Sandler SJ. 2019. Protease-deficient SOS constitutive cells have RecN-dependent cell division phenotypes. Mol Microbiol 111:405–422. https://doi.org/10.1111/mmi.14162.
46. Massoni SC, Leeson MC, Long JE, Gemme K, Mui A, Sandler SJ. 2012. Factors limiting SOS expression in log-phase cells of *Escherichia coli*. J Bacteriol 194:5325–5333. https://doi.org/10.1128/JB.00674-12.
47. Sandler SJ, Marians KJ, Zavitz KH, Coutu J, Parent MA, Clark AJ. 1999. *dnaC* mutations suppress defects in DNA replication- and recombination-associated functions in *priB* and *priC* double mutants in *Escherichia coli* K-12. Mol Microbiol 34:91–101. https://doi.org/10.1046/j.1365-2958.1999.01576.x.
48. Kuzminov A, Stahl FW. 1997. Stability of linear DNA in *recA* mutant *Escherichia coli* cells reflects ongoing chromosomal DNA degradation. J Bacteriol 179:880–888. https://doi.org/10.1128/jb.179.3.880-888.1997.
49. Skarstad K, Boye E. 1993. Degradation of individual chromosomes in *recA* mutants of *Escherichia coli*. J Bacteriol 175:5505–5509. https://doi.org/10.1128/jb.175.17.5505-5509.1993.
50. White MA, Eykelenboom JK, Lopez-Vernaza MA, Wilson E, Leach DRF. 2008. Non-random segregation of sister chromosomes in *Escherichia coli*. Nature 455:1248–1250. https://doi.org/10.1038/nature07282.
51. Kreuzer KN. 2000. Recombination-dependent DNA replication in phage T4. Trends Biochem Sci 25:165–173. https://doi.org/10.1016/s0968-0004(00)01559-0.
52. Windgassen TA, Leroux M, Sandler SJ, Keck JL. 2019. Function of a strand-separation pin element in the PriA DNA replication restart helicase. J Biol Chem 294:2801–2814. https://doi.org/10.1074/jbc.RA118.006870.
53. Willetts NS, Clark AJ, Low B. 1969. Genetic location of certain mutations conferring recombination deficiency in *Escherichia coli*. J Bacteriol 97:244–249. https://doi.org/10.1128/JB.97.1.244-249.1969.
54. Datsenko KA, Wanner BL. 2000. One-step inactivation of chromosomal genes in *Escherichia coli* K-12 using PCR products. Proc Natl Acad Sci U S A 97:6640–6645. https://doi.org/10.1073/pnas.120163297.
55. Blank K, Hensel M, Gerlach RG. 2011. Rapid and highly efficient method for scarless mutagenesis within the *Salmonella enterica* chromosome. PLoS One 6:e15763. https://doi.org/10.1371/journal.pone.0015763.
56. Cherepanov PP, Wackernagel W. 1995. Gene disruption in *Escherichia coli*: TcR and KmR cassettes with the option of Flp-catalyzed excision of the antibiotic-resistance determinant. Gene 158:9–14. https://doi.org/10.1016/0378-1119(95)00193-a.
57. Paintdakhi A, Parry B, Campos M, Irnov I, Elf J, Surovtsev I, Jacobs-Wagner C. 2016. Oufti: an integrated software package for high-accuracy, high-throughput quantitative microscopy analysis. Mol Microbiol 99:767–777. https://doi.org/10.1111/mmi.13264.
58. Stylianidou S, Brennan C, Nissen SB, Kuwada NJ, Wiggins PA. 2016. SuperSegger: robust image segmentation, analysis and lineage tracking of bacterial cells. Mol Microbiol 102:690–700. https://doi.org/10.1111/mmi.13486.